loop length between pinning points from which dislocations break away under the influence of an applied stress); Γ is the effective breakaway stress of dislocations from pinning points and is given by

$$\Gamma = \pi f_m / 4bL_c, \tag{2}$$

where f_m is the maximum binding force[8] between point defects and dislocations, and b is Burger's vector.

In the expression (2), however, the applied stress acting on the dislocation is considered to be static (low-frequency approximation). If the dynamic effect of dislocation motion under the influence of an oscillatory stress is considered, as discussed by Mason,[9,10] one has to modify the expression (2), and the corresponding expression for Γ becomes

$$\Gamma' \cong \frac{\pi f_m}{4bL_c}\left\{1+\left(\frac{\omega B/A}{\omega_0^{\,2}}\right)^2\right\}^{1/2}, \tag{3}$$

where B is the damping constant, $A \simeq \pi\rho b^2$ is the effective mass of a dislocation per unit length, $\omega_0 = (\pi/L_c)(C/A)^{1/2}$ is the resonant frequency of dislocation of loop length L_c, and C is the line tension of a dislocation. For a given frequency ω, Γ' increases with increasing damping constant B. Since the damping constant is expected to be larger in the normal state than in the superconducting state, the maximum in the attenuation is expected to occur at a higher amplitude in the normal state than in the superconducting state.

It should be emphasized that the observed amplitude dependence in both states is also of strong importance in ultrasonic determinations of the superconducting energy gap. It has been customary in these determinations to assume that the "residual" attenuation (not due to electrons) is temperature independent and is the same for the normal and for the superconducting state. The results presented here indicate that neither of these assumptions is necessarily correct.

---

*Research supported in part by Research and Technology Division, Air Force Systems Command, U. S. Air Force.

† National Aeronautics and Space Administration Trainee.

[1]R. E. Love and R. W. Shaw, Rev. Mod. Phys. 34, 260 (1964).

[2]R. E. Love, R. W. Shaw, and W. A. Fate, Phys. Rev. 138, A1453 (1965).

[3]B. R. Tittmann and H. E. Bömmel, Phys. Rev. Letters 14, 296 (1965).

[4]Raoul Weil and A. W. Lawson, Phys. Rev. 141, 452 (1966).

[5]A. Hikata, B. B. Chick, and C. Elbaum, J. Appl. Phys. 36, 229 (1965).

[6]D. H. Rogers, J. Appl. Phys. 33, 781 (1962).

[7]A. Granato and K. Lücke, J. Appl. Phys. 27, 583 (1956).

[8]A. H. Cottrell, Dislocations and Plastic Flow in Crystals (Oxford University Press, New York, 1953).

[9]W. P. Mason, Appl. Phys. Letters 6, 111 (1965).

[10]W. P. Mason, Phys. Rev. 143, 229 (1966).

METALLIC CONDUCTIVITY AND SUPERCONDUCTIVITY IN SOME SILVER CLATHRATE SALTS*

M. B. Robin, K. Andres, T. H. Geballe, N. A. Kuebler, and D. B. McWhan
Bell Telephone Laboratories, Murray Hill, New Jersey

(Received 24 August 1966)

The argentic oxide salts $(Ag_7O_8)^+X^-$ are cage structures (clathrates[1]) which consist of face-sharing Ag_6O_8 polyhedra containing the X^- anions at their centers.[2,3] We find the salts with X^- equal to NO_3^-, F^-, and BF_4^- to be the first examples of clathrates which exhibit metallic conductivity, and, in fact, we find them to be superconducting at 1.04, 0.3, and 0.15°K, respectively. In addition, the electrical resistivity of $Ag_7O_8NO_3$ as a function of temperature shows several anomalies, with abrupt changes at 220, 180, and 110°K, the second of which corresponds to a transition from a cubic lattice to a tetragonal one.

The clathrates were prepared by electrolytic oxidation of aqueous solutions of the silver salts AgX. The product in each case was either a fine powder of shiny black octahedra or centimeter-long needles, depending upon whether the electrolysis was conducted at a low current density (Pt-foil anode) or a high current density (Pt-wire anode).[4] Chemical analysis of the silver content of the salts agreed with the calculated values to within 0.2%.

X-ray-diffraction powder patterns of the three salts showed that they were cubic, the room-temperature lattice constants of the fluoride, nitrate, and the hitherto unreported fluoborate being 9.833 ± 0.002, 9.893 ± 0.002, and 9.942 ± 0.004 Å, respectively. The visually estimated intensities for $Ag_7O_8NO_3$ are in agreement with those calculated for the proposed structure.[2,3] Powder patterns of $Ag_7O_8NO_3$ recorded at various temperatures show that at a point near but below 200°K, the salt undergoes a transition from a cubic lattice to a tetragonal one having $c/a = 0.9603$ at 10°K. The ratio of lattice constants for this salt at 10 and 298°K are $a_{10}/a_{298} = 1.0109 \pm 0.0004$ and $c_{10}/a_{298} = 0.9704 \pm 0.0004$. Since the oxygens of the four NO_3^- groups must be statistically distributed over the 96-fold position in the cubic phase, it seems reasonable to assume that the transition to the tetragonal phase involves the alignment of the planes of the NO_3^- groups perpendicular to the c axis. In accord with such a suggestion, the fluoride and fluoborate salts, which contain more spherical anions than the nitrate salt, were found to remain cubic when cooled to 10 and 77°K, respectively.

A typical curve of resistivity versus temperature for a single crystal of $Ag_7O_8NO_3$ is shown in Fig. 1.[5] Abrupt changes in resistivity are observed at approximately 220, 180, and 110°K, the anomaly at 180°K consisting sometimes of an increase and sometimes of a decrease of resistivity with decreasing temperature. Residual resistivity ratios, $\rho(300°)/\rho(4.2°)$, as large as 200 were observed for the nitrate salt, the phonon resistivity $\rho(T)-\rho(1.1°)$ increasing roughly as $T^{3.5}$ up to 12°K, and less rapidly above this temperature. The sometimes positive, sometimes negative resistivity change observed on going through the 180°K transition can be explained as due to a variation in the relative amounts of a- and c-axis-oriented material which is aligned along the needle axis following the crystallographic transition.

Regardless of crystal morphology, $Ag_7O_8NO_3$ becomes superconducting at 1.04°K, with the needles showing the sharper transition (0.04° wide). The superconducting transitions in the fluoride and fluoborate salts were broader than that in the nitrate and were observed at 0.3 and 0.15°K, respectively. A mixed crystal containing 75 anion-mole% NO_3^- and 25 anion-mole% F^- went superconducting in the interval 0.85-0.90°K, indicating a linear relationship between the superconducting transition temperature and the mole% F^- in the NO_3^- salt.

We have investigated the superconductivity of the nitrate salt in some detail, having measured its magnetization curve in the superconducting state at 0.1°K by observing the Meissner effect as a function of field. The measurements were carried out by warming and cooling the sample in constant fields from 0.1 to above 1.04°K and observing the reversible entry and expulsion of flux ballistically. The result, shown in Fig. 2, is typical of a type-II superconductor with a high value of the Landau-Ginzberg parameter κ. In contrast to the case of a "dirty" superconductor, the large value of κ measured here (approximately 100) probably results from a large penetration depth rather than from a small coherence length. From the area under the magnetization curve,

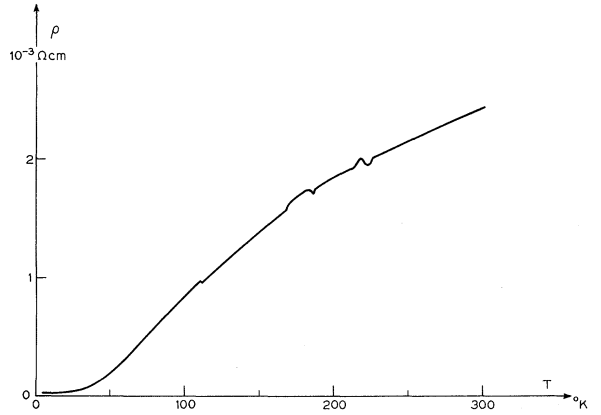

FIG. 1. The temperature-resistivity curve for a single crystal of $Ag_7O_8NO_3$.

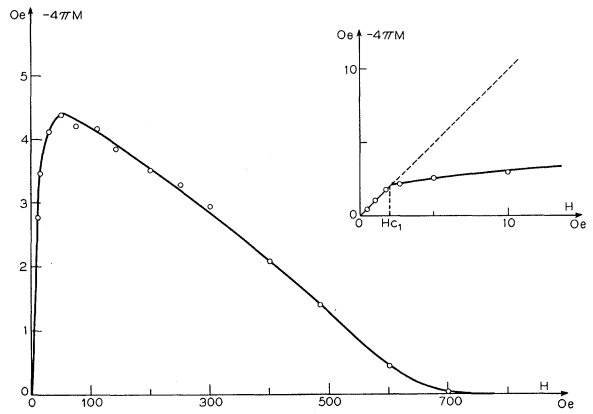

FIG. 2. Magnetization curve of powdered $Ag_7O_8NO_3$ at 0.1°K.

we compute a thermodynamic critical field of 57 Oe. Assuming a parabolic critical field curve, we compute from this an electronic specific heat, γ, equal to 0.050 mJ/cm^3 °K^2. Though this value is close to that for metallic silver (0.065 mJ/cm^3 °K^2), it is clear that the conduction bands must be much narrower and the effective masses much larger in the clathrate than in metallic silver, since the electron density is undoubtedly much lower in the clathrate.

The fact that the superconducting transition temperature of the nitrate salt is three to six times as high as those of the fluoride and fluoborate salts suggests that isotope effect experiments might give useful information. Such experiments are under way.

We would like to thank G. W. Hull, Jr., Mrs. Ann Cooper, and S. Cunningham for help with the measurements, and B. T. Matthias for being our devil's advocate.

[1]H. M. Powell, J. Chem. Soc. 1948, 61.
[2]Chou Kung-Du, Scientia Sinica (Peking) 12, 139 (1963).
[3]I. Náray-Szabó, G. Argay, and P. Szabó, Acta Cryst. 19, 180 (1965).
[4]I. Náray-Szabó and K. Popp, Zeit. Anorg. Allgem. Chem. 322, 286 (1963).
[5]J. A. McMillan, Chem. Rev. 62, 65 (1962), states that he has observed $Ag_7O_8NO_3$ to exhibit semiconductivity, but gives no details.

RELATIVE QUANTUM YIELD FOR PHOTOEMISSION FROM THIN FILMS OF XENON AND KRYPTON

J. F. O'Brien and K. J. Teegarden*
Institute of Optics, University of Rochester, Rochester, New York
(Received 22 September 1966)

The photoelectric yield for thin films of xenon and krypton has been studied from 7.5 to 11.7 eV. For solid xenon a direct emission threshold is observed at 9.7 eV, and the electron affinity is estimated to be 0.39 eV. No threshold occurs in krypton below 11.7 eV, but emission associated with defect centers is observed below threshold in both materials. Measurement of the energy distribution of the emitted electrons could not be made because of strong polarization effects produced by the electron emission.

The experimental equipment has been described elsewhere.[1,2] The cryostat was isolated from the monochromator by a lithium fluoride window and pumped to a base pressure of 5×10^{-9} Torr by a Vac-Ion pump. The samples were deposited on substrates at 20°K, and film thicknesses of several hundred angstroms were estimated from comparison with the absorption data taken by Baldini,[3] shown in Fig. 1. Since the films were polarized by the emission of electrons, all data were taken at low light intensities and at voltages far above the saturation level.

Figure 2 is a curve of the quantum yield, in

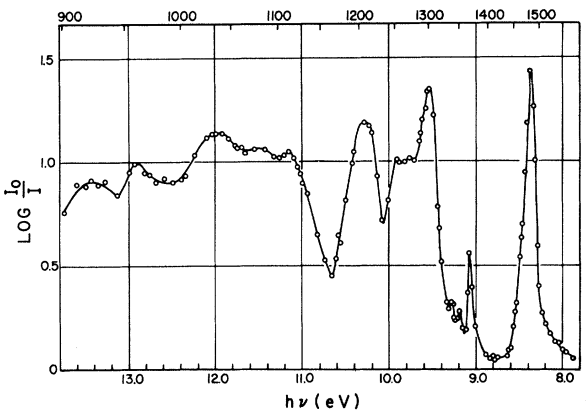

FIG. 1. Absorption spectrum of solid Xe at 12°K (annealed at 53°K), after Baldini.[3]

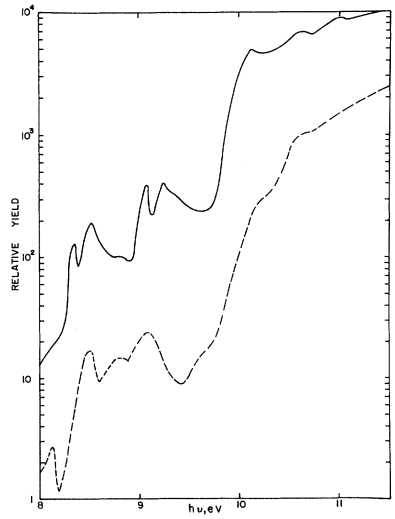

FIG. 2. Relative quantum yield in arbitrary units of solid Xe at 20°K on a Pt substrate. Unannealed film (dashed). Film annealed at 55°K (solid).